D-6-3
Extended Abstracts of the 2015 International Conference on Solid State Devices and Materials, Sapporo, 2015, pp742-743

Structural and Magnetic Characterizations of Vertical Ferromagnetic MnAs/Semiconducting InAs Heterojunction Nanowires

Ryutaro Kodaira, Kyohei Kabamoto, Shinya Sakita, and Shinjiro Hara

Research Center for Integrated Quantum Electronics, Hokkaido University
North 13 West 8, Sapporo 060-8628, Japan
Phone: +81-11-706-7172, E-mail: kodaira@rciqe.hokudai.ac.jp

Abstract

We fabricate free-standing nanowires (NW) with vertical heterojunction between ferromagnetic MnAs/Semiconducting InAs on GaAs (111)B substrates by selective-area metal-organic vapor phase epitaxy of free-standing InAs NWs and endotaxial MnAs nanoclustering. Marked single magnetic domains are observed in ferromagnetic MnAs nanoclusters (NC) in InAs NWs. Structural characterizations reveal that the positions, size, and number of NCs in NWs strongly depend on growth conditions for the NC formation.

1. Introduction

Vertical free-standing semiconducting nanowires (NW) are of extraordinary interests for potential applications to next-generation electronic, photonic, and bio-chemical sensing devices. We have demonstrated III-V compound semiconducting NWs by using selective-area metal-organic vapor phase epitaxy (SA-MOVPE) [1], which is a catalyst-free and bottom-up fabrication technique with a high degree of controllability in the position, size, aspect ratio, and density of NWs on various types of semiconducting substrates. We successfully created vertical surrounding gate field-effect transistors (VSG-FET) using our semiconducting NWs grown by SA-MOVPE [2]. The VSG-FETs possess advantageous device characteristics, e.g., superior transconductance, high current on-off ratio, and suppressed short-channel effects. In our previous studies, we have recently been demonstrating the synthesis of hybridized structure between ferromagnetic MnAs nanoclusters (NC) and semiconducting NWs [3]. This hybridized structure is offering a new possibility and versatility for creating novel nanospintronic devices, such as spin-NW-MOSFETs. A high degree of controllability in the MnAs NC formation and ferromagnetic characteristics in the NWs is required to create such a novel nanospintronic device. In this paper, therefore, we report on the detailed growth condition dependences of the MnAs NC formation in the host InAs NWs. Magnetic characterization results by magnetic force microscopy (MFM) are also described.

2. Experimental Procedure

First, we prepared the initial circular openings, which were arranged and defined in SiO_2 thin films by electron beam lithography. The distances between the initial circular openings, or the periods, *a*, were 0.5, 1.0, and 3.0 μm. The SiO_2 thin films, whose typical thickness was estimated to be approximately 20 to 30 nm, were deposited on GaAs (111)B wafers by plasma spattering. The growth temperature, T_g, and the growth time, *t*, for InAs NWs were 580 °C and 30 min, respectively. The estimated partial pressures of $(CH_3)_3In$ and 20%-AsH_3 diluted in H_2 were 4.9 x 10^{-7} and 1.3 x 10^{-4} atm, respectively, for the SA- MOVPE of undoped InAs NW templates. For the MnAs NC growth after the NW growth, we utilized the phenomenon of “endotaxy”. During the endotaxy, we only supplied the organometallic source of $(CH_3C_5H_4)_2Mn$ diluted in H_2. For the MnAs NCs, T_g were changed from 400 to 580 °C, and *t* were 1, 2, and 5 min. The estimated partial pressure of $(CH_3C_5H_4)_2Mn$ was 5.2 x 10^{-4} atm. During the decrease in temperature in the purging process after the MnAs NC growth, 20 %-AsH_3 diluted in H_2 was supplied. Structural characterizations were carried out by scanning electron microscopy (SEM). Transmission electron microscopy (TEM) was also used for observing lattice images of the NCs and NWs, and we conducted the analyses of crystal structures and solid compositions of the NCs and NWs by electron-beam diffraction (ED) and energy dispersive X-ray (EDX) spectroscopy in combination with TEM. For the magnetic characterization of MnAs NCs, we used MFM at room temperature after applying the external magnetic fields, ***B***, of approximately 5,700 Gauss.

3. Results and Discussion

Figures 1(a) and 1(b) show a highly-magnified cross-sectional TEM image for the MnAs NC formed in the middle part of the InAs NW and a lattice image around the interface between NC and NW, respectively. The MnAs NCs in the NWs were grown at 580 °C for 1 min. Figure 1(a) revealed that the double heterojunction between MnAs and InAs was formed in the NWs. The result was consistent with the EDX analyses for the solid compositions (not shown here). In addition, we observed that atomically-abrupt heterointerfaces between MnAs NCs and InAs NWs were formed, as shown in Fig. 1(b). We concluded from the ED patterns that the MnAs NCs and the InAs NWs had the hexagonal NiAs-type and zinc-blende-type crystal structures, respectively (not shown here). The c-axes, i.e., the <0001> directions, of the NiAs-type MnAs NCs were approximately parallel to the <111>B directions of the zinc-blende-type InAs NWs.

Subsequently, we conducted MFM observation for one of the heterojunction NWs after applying the ***B***. Figures 1(c) and 1(d) show the SEM and MFM images of a typical heterojunction NW, respectively. The insets show the highly-magnified images for the NC “*A*” indicated by a white circle. It was highly possible, from the TEM observation results shown in Figs. 1(a) and 1(b), that the NC "*A*" penetrated through the InAs NWs with atomically-abrupt heterointerfaces. It was likely, therefore, that the c-axis of the NC "*A*" was parallel to the <111>B direction of InAs NWs. In this case, the magnetic easy axes of MnAs NCs, i.e., a-axes, are perpendicular to the <111>B direction, as shown in Fig. 2(a). Figure 1(d) showed that some of the MnAs NCs had marked single magnetic domains, and revealed that the NC "*A*" was magnetized possibly along one of the a-axes, which was presumably parallel to the ***B*** direction, as explained in Fig. 2(b) for the observed bright and dark contrasts in Fig. 1(d).

To discuss the NC formation, next, we measured the average size of NCs formed on the top {111}B crystal facets, W_{ct}, and vertical distance between the NCs, D_c. Figure 3(a) summarizes the T_g dependence of the average W_{ct} and D_c, and the inset SEM image shows the definition of them. As shown in Fig. 3(a), both W_{ct} and D_c markedly increased with increasing T_g. That possibly suggests that the surface migration length of manganese atoms adsorbed on the InAs NW surfaces is one of the key factors in the MnAs NC formation. Substitution reactions from indium atoms to manganese ad-atoms result in the NC growth after the surface migration of manganese ad-atoms. The longer the surface migration length becomes at higher T_g, the more the manganese ad-atoms possibly reach to one certain chemical adsorption site. This leads to the increase in both W_{ct} and D_c.

Next, Figure 3(b) shows the dependences of average NW heights on the period, *a*, of the host InAs NWs before and after the MnAs NC formation. The MnAs NCs were grown at 580 °C for 1 min. We observed that both height of NWs and number of NCs decreased with decreasing *a*, as shown in Fig. 3(b) and the insets. In the case of small *a*, more of the manganese ad-atoms possibly reach to one certain chemical adsorption site because the surface migration length is long enough compared with the NW height. Therefore, the shorter in height the NWs were grown, the fewer the NCs were formed. In addition, we observed that the average heights of NWs increased with increasing the number of NCs. These results suggest that the number of NCs was strongly affected by the NW heights and the surface migration length of manganese ad-atoms. For the NWs, in which no NC was formed in their middle part, the average height of NWs was approximately 600 nm. It was possible, therefore, that the surface migration length of manganese ad-atoms at T_g of 580 °C was roughly estimated to be 600 nm at least. It seemed that these analyses and discussion were consistent with the experimental results shown in Fig. 3(a), because the D_c obtained for the NCs grown at 580 °C was approximately 600 nm.

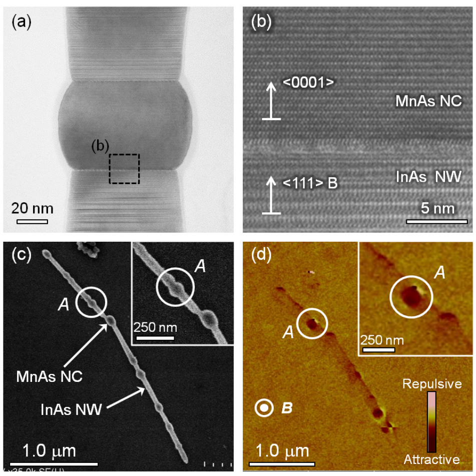

Fig. 1 (a) Highly-magnified TEM image for the MnAs NCs formed in the middle part of InAs NW and (b) lattice image for a heterointerface between MnAs and InAs layers. (c) SEM and (d) MFM images for one of the ferromagnetic MnAs/semiconducting InAs heterojunction NWs.

4. Conclusions

We fabricated the vertical ferromagnetic MnAs/semiconducting InAs heterojunction NWs with atomically-abrupt heterointerfaces. The detailed growth condition dependences revealed that the parameters, T_g for the NCs and *a* for the NW templates were the key factors in the formation of MnAs NCs with a single magnetic domain into the InAs NWs to control the position, size, and number of the NCs in the NWs.

Acknowledgements

The authors thank Dr. M. T. Elm, Prof. P. J. Klar, Prof. T. Fukui, and Prof. J. Motohisa for fruitful discussions.

References

[1] J. Noborisaka *et al.*, Appl. Phys. Lett. **87**, 093109 (2005)
[2] T. Tanaka *et al.*, Appl. Phys. Express **3**, 025003 (2010)
[3] S. Hara *et al.*, Jpn. J. Appl. Phys. **51**, 11PE01 (2012)

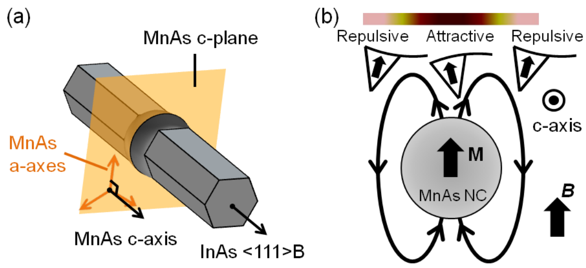

Fig. 2 Schematic illustrations for (a) the crystal axis relationship in the heterojunction NWs and (b) the magnetic response from the MnAs NC in the MFM observations.

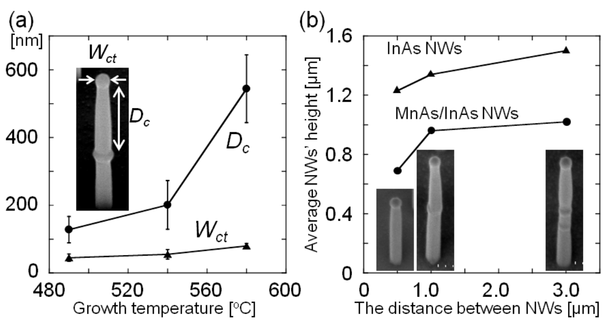

Fig. 3 Dependences of the MnAs NC formation in the InAs NWs on (a) T_g for the NCs and (b) *a* for the NWs. The inset in (a) shows a typical heterojunction NW at 580 °C.